Functional Estimation of Loop−Helix Boundaries in the Lactose Permease of *Escherichia coli* by Single Amino Acid Deletion Analysis†

Christopher D. Wolin and H. Ronald Kaback*

Howard Hughes Medical Institute, Departments of Physiology and Microbiology & Molecular Genetics, Molecular Biology Institute, University of California, Los Angeles, Los Angeles, California 90025-1662

Received November 8, 2000; Revised Manuscript Received December 11, 2000

ABSTRACT: Mutants with single amino acid deletions in the loops of lactose permease retain activity, while mutants with single deletions in transmembrane helices are inactive, and the loop−helix boundaries of helices IV, V, VII, VIII, and IX have been approximated functionally by the systematic deletion of single residues [Wolin, C. D., and Kaback, H. R. (1999) *Biochemistry 38*, 8590−8597]. The experimental approach is applied here to the remainder of the permease. Periplasmic and cytoplasmic loop−helix boundaries for helices I, II, X, XI, and XII and the cytoplasmic boundary of helix III are in reasonable agreement with structural predictions. In contrast, the periplasmic end of helix III appears to be five to eight residues further into the transmembrane domain than predicted. Taken together with the previous findings, the analysis estimates that 11 of the 12 transmembrane helices have an average length of 21 residues. Surprisingly, deletion analysis of loop V/VI, helix VI, and loop VI/VII does not yield an activity profile typical of the rest of the protein, as individual deletion of only three residues in this region abolishes activity. Thus, transmembrane domain VI which is probably on the periphery of the 12-helix bundle may make few functionally important contacts.

Hydropathy analysis (*1*) and more sophisticated algorithms (reviewed in *2*) predict that the lactose permease (lac permease)[1] of *Escherichia coli* contains 12 transmembrane domains that traverse the membrane in zigzag fashion connected by relatively hydrophilic loops with both N and C termini on the cytoplasmic face (Figure 1). A large body of experimental evidence which includes studies on an extensive series of lac permease−alkaline phosphatase fusions (*3*) supports the general features of the model (reviewed in *4*, *5*). However, with the exceptions of the C terminus (*6*−*9*) and periplasmic loop VII/VIII (*10*−*12*), the helix−loop boundaries were based almost entirely on predictive algorithms.

In this context, it is important that predictive algorithms do not take into account charge pairing. Thus, when mutagenesis and chemical rescue experiments indicated that Asp237 and Asp240 in helix VII are charge paired with Lys358 (helix XI) and Lys319 (helix X), respectively (*13*−*19*), the secondary structure was altered to include Asp237 and Asp240 within helix VII (*15*), and subsequently, more direct evidence for the modification was presented (*10*, *12*, *20*, *21*). In a similar vein, Glu126 (helix IV) and Arg144 (helix V) were predicted to be at the membrane−water interface at the cytoplasmic face of the membrane (*1*). However, in addition to playing a critical role in substrate binding (*22*−*24*), the two residues are in close proximity (*25*, *26*) within the plane of the membrane (*27*, *28*).

While integral membrane proteins generally tolerate point mutations relatively well (*29*−*32*), insertion or deletion mutations appear to be disruptive in transmembrane helical domains (*29*, *30*, *32*), but not in extramembranous loops (*29*, *30*, *32*, *33*). Based on the postulate that insertion of a single amino acid at any position within a transmembrane helix should be disruptive if contacts with neighboring helices are important for activity, Braun et al. (*34*) studied lac permease by inserting Ala residues primarily into transmembrane domain III.

To approximate helix−loop boundaries functionally, we chose to delete single amino acid residues from lac permease systematically, the general idea being that like insertions, deletions should be disruptive to transmembrane helices, but relatively innocuous in loops (*27*). Beginning with loop VII/VIII, the N terminus of which has been clearly delineated (*10*, *12*), it was shown that single or multiple deletions have relatively little effect on permease activity. On the other hand, deletion of single amino acid residues over a narrow range of positions near the loop−helix boundary leads to marked loss of activity. Based on these observations within a defined region of the permease, other domains were studied. Findings consistent with predictive algorithms were obtained in loops VI/VII, VIII/IX, and IX/X and the flanking helices. However, deletion analysis of loops III/IV, IV/V, and V/VI and the flanking helices indicates that Glu126 and Arg144 are located within helices IV and V as shown by nitroxide-scanning electron spin resonance spectroscopy (*28*). The study lends credance to the notion that single amino acid deletions may be used to approximate loop−helix boundaries in a functional manner.

† This work was supported in part by NIH Grant DK51131 to H.R.K.

* Correspondence should be addressed to this author at HHMI/UCLA, 6-720 MacDonald Building, P.O. 951662, 675 Circle Dr., Los Angeles, CA 90095-1662. Telephone: (310) 206-5053. Telefax: (310) 206-8623. E-mail: RonaldK@HHMI.UCLA.edu.

[1] Abbreviations: lac, lactose, lactose permease; Δ, deletion.

10.1021/bi0025767 CCC: $20.00
Published on Web 01/26/2001

In this paper, single amino acid deletion analysis is applied to the N and C termini, as well as the remaining loops in the permease. The boundaries estimated for both termini, loops I/II, II/III, X/XI, and XI/XII, and the flanking helices are in reasonably good agreement with the predicted topology. However, analysis of loop III/IV suggests that helix III may be significantly shorter than predicted. Remarkably, individual deletion of only three residues in putative transmembrane domain VI leads to complete inactivation, thereby highlighting this domain for further study.

EXPERIMENTAL PROCEDURES

Materials. Oligonucleotides were synthesized on an Applied Biosystems 381A DNA synthesizer. [1-^{14}C]Lactose and ^{125}I-labeled Protein A were obtained from Amersham (Sunnyvale, CA). Restriction endonucleases, T4 DNA ligase, and appropriate reaction buffers were from New England Biolabs (Beverly, MA). Sequenase (modified T7 polymerase) and Sequence reaction kits were from United States Biochemicals (Cleveland, OH). Elongase Enzyme Mix and buffer was obtained from Gibco BRL (Gaithersburg, MD). Site-directed rabbit polyclonal antiserum against a dodecapeptide corresponding to the C terminus of permease (*35*) was prepared by BabCo (Richmond, CA). Deoxyoligonucleotides were synthesized on an Applied Biosystems 381A DNA synthesizer. All other materials were reagent grade obtained from commercial sources.

Bacterial Strains and Plasmids. Subcloning grade *E. coli* XL-1blue [F′:: Tn10 *proA*$^+$*B*$^+$ *lacI*^{q} Δ*(lacZ)*M15*/ recA*1 *endA*1 *gyr*A96 (Nal^r) *thi hsd*R17 ($r_k^-m_k^+$) *sup* E44 *rel* A1 *lac*] (Stratagene Cloning Systems, Inc., La Jolla, CA) was used as a host for transformation of all PCR products and subcloning procedures. *E. coli* HB101 [F− Δ(*gpt-proA*) *leuB*6 *sup*E44 *ara*-14 *gal*k2 *lacY*1 Δ(*mcr*C-*mmr*) *rps*L20 *xyl*-5 *mtl*-1 *recA*13] (Promega, Inc., Madison, WI) was used for initial assessment of permease activity by growth on MacConkey indicator plates containing lactose. *E. coli* T184 [F′ *lacI*^{q}*O*$^+$*Z*^{U118} (*lacY*$^+$*lacA*$^+$) /*lacI*$^+$*O*$^+$*Z*$^-$*Y*$^-$(*A*$^+$), *rps*L *met thr recA hsd*MR] was used for expression of lac permease and active transport assays. For increased expression of lac permease, T184 were lysogenized with λ DE3 phage which contains the T7 polymease gene (Novagen, Inc., Madison, WI). All deletion mutants were created in pT7-5/cassette *lacY* (EMBL-X56095) encoding wild-type lac permease.

Construction of Deletion Mutants. Amino acid residues were deleted using a modification of the inverse polymerase chain reaction as previously described (*27*).

Colony Morphology. For qualitative assessment of permease activity, *E. coli* HB101 (*Y*$^-$*Z*$^+$) was transformed with plasmid encoding a given mutant, and the cells were plated on MacConkey indicator media containing 25 mM lactose and the phenotypes were scored as previously described (*27*).

Active Transport. Cells transformed with single deletion mutants were grown and transport assayed by rapid filtration as previously described (*27*). Rates of transport were approximated at 2 min, and the rate of transport for cells transformed with vector containing no *lacY* (ca. 2.5 nmol/mg of protein) was subtracted. The specific activities of mutants were calculated by dividing the rate of transport at 2 min (% wild-type) by expression (% wild-type). In cases where the rate and/or expression was less than 10% of wild-type, specific activities could not be determined accurately. In addition, lactose transport was determined after 60 min incubation. The average level of accumulation in T184 cells harboring pT7-5/cassette *lacY* was 125 nmol/mg of protein and 8 nmol/mg of protein for T184 cells harboring pT7-5 with no *lacY* insert. All values are expressed as a percentage of wild-type.

Quantification of Permease. Membranes were prepared from cells assayed for transport activity, and expression was quantitated by autoradiography utilizing a model 425F Phosphorimager (Molecular Dynamics) as described (*27*).

RESULTS

The N Terminus. The N terminus of helix I is predicted to begin at Phe9 (Figure 1). Single deletion mutants were constructed at the N terminus starting at Phe9 and proceeding into transmembrane domain I. When expressed in *E. coli* HB101 (*Z*$^+$*Y*$^-$), mutants Δ9, Δ10, Δ11, and Δ12 grow as red colonies on MacConkey medium containing lactose, indicating that these mutants retain significant ability to catalyze downhill lactose translocation. In contrast, mutants Δ13, Δ14, and Δ15 grow as colonies with a reddish center bordered by a white halo (i.e., "haloed"), a phenotype characteristic of decreased transport activity. All of the mutants are expressed at near-wild-type levels, as judged by quantitative immunoblots (Figure 2). For more quantitative measurements, *E. coli* T184 (*Z*$^-$*Y*$^-$) was transformed with plasmid encoding a given mutant and assayed for active lactose transport. Mutants Δ9, Δ10, and Δ11 exhibit highly significant specific activities, as well as levels of accumulation relative to wild-type permease. Although the Δ12 mutant catalyzes significant accumulation by 60 min, it displays a very low specific activity, and mutants Δ13, Δ14, and Δ15 exhibit immeasurably low specific activities. Single deletion of Leu14 or Phe15 results in mutants with little or no transport activity. Thus, based on the specific activities of the deletion mutants, the N terminus of helix I begins at Met11/Phe12.

Loop I/II. Trp33 is predicted to be the C-terminal residue in helix I, and Ile47 is predicted to be at the N terminus of helix II (Figure 1). Deletion mutant Δ32 displays a white phenotype on indicator plates, mutants Δ34 through Δ43 confer red phenotypes, and mutants Δ33, Δ44, Δ45, Δ46, and Δ47 grow as haloed colonies, and with the exception of the Δ32 mutant, the mutants are expressed at measurable levels (Figure 3). Deletion mutants Δ34 to Δ43 exhibit significant specific activities and levels of lactose accumulation at 60 min. In contrast, deletion mutants Δ33, Δ44, and Δ45 show low levels of lactose accumulation at 60 min, and Δ32, Δ46, and Δ47 are essentially inactive. Overexpression of the Δ32, Δ33, Δ46, and Δ47 in *E. coli* T184(DE3), an isogenic strain containing T7 polymerase as a λ lysogen, does not result in increased activity, indicating that loss of activity is not due to low expression levels (Table 1). Accordingly, based on these data and those presented above, helix I starts with Met11/Phe12 at the N terminus, ending with Ile32 at the C terminus with loop I/II extending from Trp33 through Thr45, both of which are within one to two residues of the predicted topology (Figure 1).

Loop II/III. Loop II/III is predicted to extend from residues Ser67 to Lys74 (Figure 1). Single deletion mutants in this

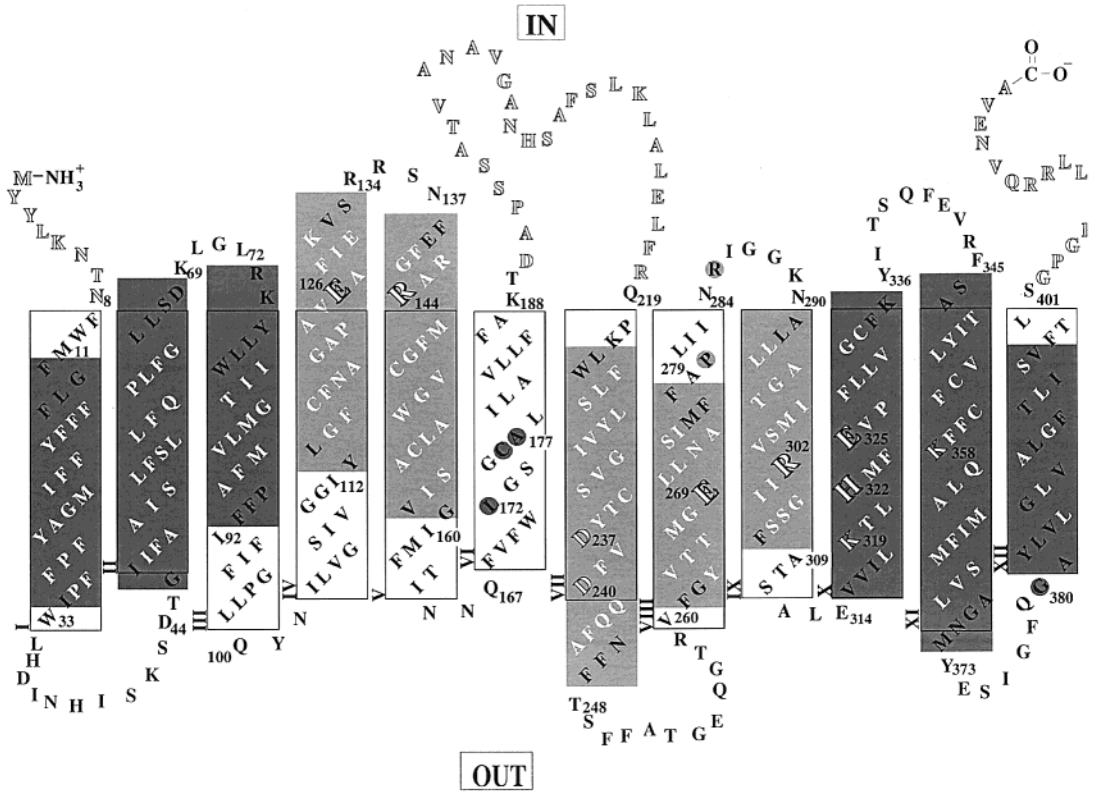

FIGURE 1: Secondary structure model of the lac permease. The single-letter amino acid code is used, residues critical for active transport are highlighted in enlarged, open faced type, and the charge pairs Asp237/Lys358 and Asp240/Lys319 are shown in open-face type. The outlined rectangles represent putative transmembrane helical regions predicted utilizing the HMMTOP Version 1.1 algorithm (*2*). Small solid letters represent amino acid residues that have been individually deleted. Shaded regions indicate transmembrane helical regions defined by single deletion analysis where the ends of the helices are placed at the first residue where activity is abolished upon deletion. The dark gray area represents results from this study, and the lightly shaded regions represent previously published results (*27*). The gray circles represent isolated residues where deletion results in loss of active transport.

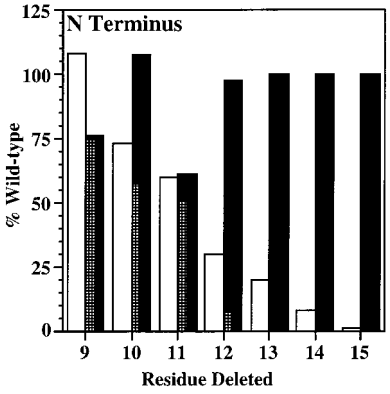

FIGURE 2: Lactose accumulation (white bars), specific activity (stippled bars), and expression (black bars) of single deletion mutants at the proposed N terminus of helix I. Active transport and expression were assayed as described under Experimental Procedures. The amino acid deleted is denoted by the position within the primary sequence.

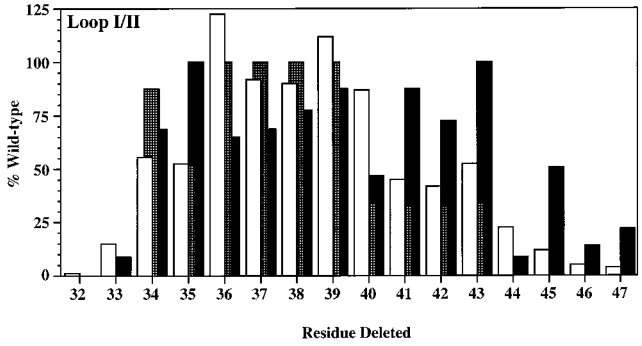

FIGURE 3: Lactose accumulation (white bars), specific activity (stippled bars), and expression (black bars) of single deletion mutants encompassing residues proposed for loop I/II. Active transport and expression were assayed as described under Experimental Procedures. The amino acid deleted is denoted by the position within the primary sequence.

region exhibit a haloed phenotype on indicator plates, and despite generally good expression, all exhibit very low specific activities (Figure 4). However, mutants Δ69 to Δ72 (with the possible exception of Δ70) accumulate lactose significantly better than the other mutants. Although it is clearly difficult to assign specific residues to loop II/III due to low activity generally, based on levels of accumulation in 60 min, the N terminus of the loop is probably at or around Asp68/Lys69 and the C terminus approximates Leu72/Arg73, which is in reasonable agreement with prediction (Figure 1). These results together with those presented above suggest that helix II is comprised of 22 to 23 residues extending from about Gly46 to Ser67 or Asp68.

Loop III/IV. The activity of single deletion mutants ΔGly110/111 through ΔLeu114 at the C terminus of loop III/IV suggests that the periplasmic end of helix IV terminates at Tyr113 and not at Ile103 as predicted (*27*). To complete analysis of this region, single deletions were constructed from Val109 toward the periplasmic end of helix III, which is predicted to terminate at Leu99 (Figure 1). Mutants Δ89−Δ109 exhibit red phenotypes indistinguishable from wild-type on indicator plates, indicating that all retain high activity

Table 1: Properties of Selected Single Deletion Mutants in *E. coli* T184(DE3)

residue deleted	expression (wt %)[a]	accumulation[b] (wt %)
	Loop I/II	
32 I	95	2.5
33 W	178	20
46 G	88	7.9
47 I	128	2.7
	Helix VI	
177 A	128	3.0
	Loop XI/XII	
369 A	137	2.0
370 G	174	4.0
371 N	144	8.0
372 A	149	5.0
380 G	170	3.0
383 L	24	2.0
384 V	162	7.0
	C Terminus	
388 V	124	4.0
390 L	150	8.0
392 F	115	8.0
394 L	92	4.0
396 S	177	18
397 V	166	27

[a] wt, wild-type. [b] Transport at 60 min.

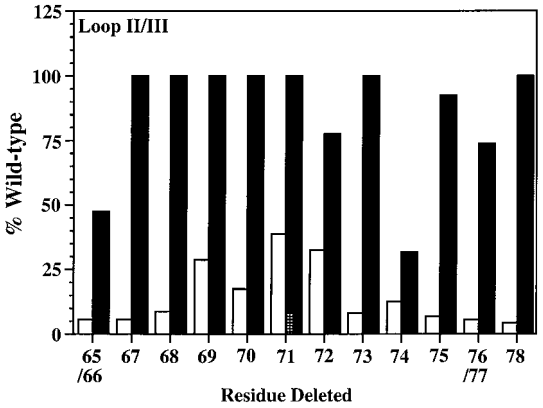

FIGURE 4: Lactose accumulation (white bars), specific activity (stippled bars), and expression (black bars) of single deletion mutants encompassing residues proposed for loop II/III. Active transport and expression were assayed as described under Experimental Procedures. The amino acid deleted is denoted by the position within the primary sequence. In cases where identical amino acids occur sequentially, deletion of one of the residues is indicated by listing both positions separated by a slash.

with respect to downhill lactose transport. Moreover, each mutant is expressed to a significant level as judged by quantitative immunoblots (Figure 5). When the mutants are assayed for active transport, with the exception of Δ89 and Δ90/91, mutants Δ92 to Δ109 transport lactose with relatively high specific activities to significant levels of accumulation. Thus, loop III/IV appears to contain 21 residues from Ile92 to Ile112, and helix III is comprised apparently of 18 to 19 residues extending from Arg73/Lys74 to Phe91, conclusions that differ significantly from the predicted secondary structure (Figure 1).

Loop V/VI, Helix VI, and Loop VI/VII. The activity pattern of deletion mutants ΔVal158 through ΔPhe162 at the N terminus of loop V/VI suggests that the last residue at the periplasmic end of helix V is Gly159 rather than Ile164 (*27*). Putative helix VI is predicted to extend from Phe168 to

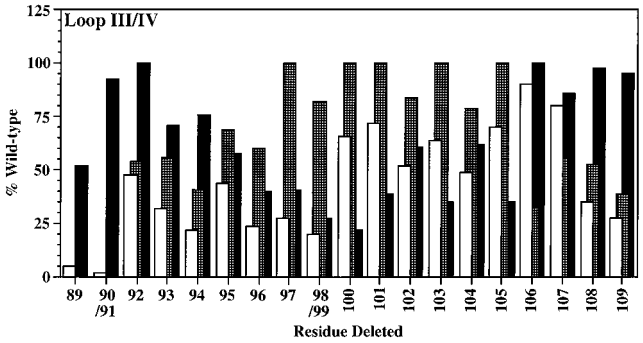

FIGURE 5: Lactose accumulation (white bars), specific activity (stippled bars), and expression (black bars) of single deletion mutants encompassing residues proposed for loop III/IV. Active transport and expression were assayed as described under Experimental Procedures. The amino acid deleted is denoted by the position within the primary sequence. In cases where identical amino acids occur sequentially, deletion of one of the residues is indicated by listing both positions separated by a slash.

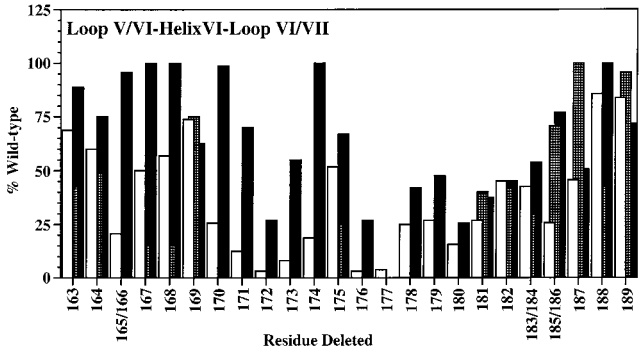

FIGURE 6: Lactose accumulation (white bars), specific activity (stippled bars), and expression (black bars) of single deletion mutants encompassing residues proposed for loop V/VI, helix VI, and loop VI/VII. Active transport and expression were assayed as described under Experimental Procedures. The amino acid deleted is denoted by the position within the primary sequence. In cases where identical amino acids occur sequentially, deletion of one of the residues is indicated by listing both positions separated by a slash.

Ala187 (Figure 1). To approximate the boundaries of this domain, mutants Δ163 to Δ189 were constructed.

Mutants Δ163 to Δ169 in putative periplasmic loop V/VI, as well as Δ188 and Δ189 in putative cytoplasmic loop VI/VII, grow as red colonies on indicator plates, and mutants Δ170 to Δ175 and Δ178 to Δ187, all of which are predicted to be within putative helix VI, confer haloed phenotypes. Mutants Δ176 and Δ177 grow as white colonies on indicator media. Thus, based on downhill lactose translocation, the pattern observed is consistent with the loop−helix boundaries predicted for this region (Figure 1). In addition, with the exception of Δ177, all of the mutants are expressed at measurable levels (Figure 6). However, when active transport is assayed, no identifiable pattern is observed for either specific activity or accumulation in 60 min. Thus, with the exceptions of mutants Δ171−Δ173, Δ176, and Δ177 which exhibit little or no activity, all of the other deletion mutants catalyze active lactose transport with significant specific activities and/or levels of accumulation. Furthermore, expression of mutant Δ177 in *E. coli* T184(DE3) does not result in increased lactose accumulation (Table 1).

Loop X/XI. The previous study (*27*) indicates that Val315 represents the N terminus of helix X (Figure 1). To estimate

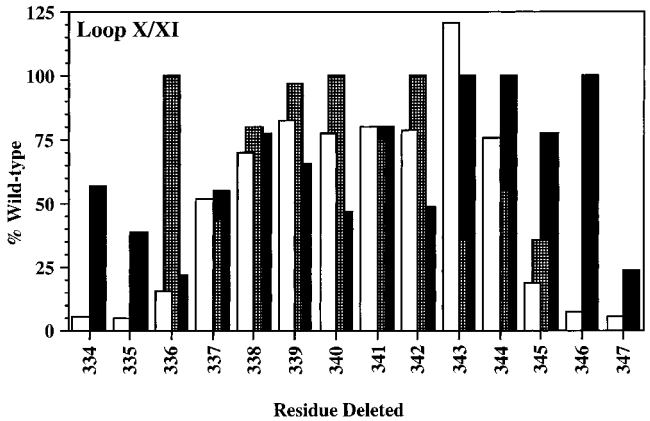

FIGURE 7: Lactose accumulation (white bars), specific activity (stippled bars), and expression (black bars) of single deletion mutants encompassing residues proposed for loop X/XI. Active transport and expression were assayed as described under Experimental Procedures. The amino acid deleted is denoted by the position within the primary sequence.

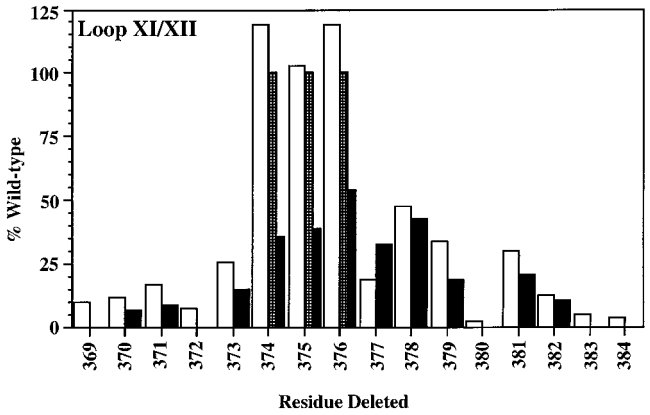

FIGURE 8: Lactose accumulation (white bars), specific activity (stippled bars), and expression (black bars) of single deletion mutants encompassing residues proposed for loop XI/XII. Active transport and expression were assayed as described under Experimental Procedures. The amino acid deleted is denoted by the position within the primary sequence.

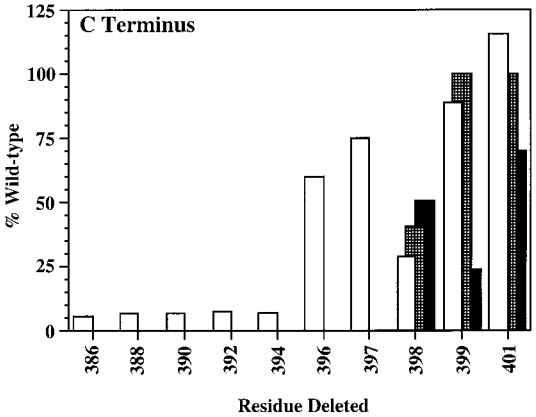

FIGURE 9: Lactose accumulation (white bars), specific activity (stippled bars), and expression (black bars) of single deletion mutants encompassing residues proposed for helix XII and the C terminus. Active transport and expression were assayed as described under Experimental Procedures. The amino acid deleted is denoted by the position within the primary sequence.

the cytoplasmic boundaries of helices X and XI, deletion mutants extending from Phe334 through Ala347 were constructed. Mutants Δ334 to Δ337 display a haloed phenotype, mutants Δ338 to Δ344 a red phenotype indistinguishable from wild-type, mutants Δ345 and Δ346 a haloed phenotype, and mutant Δ347 grows as white colonies. All of the mutants are expressed at measurable levels (Figure 7). With respect to active transport, mutants Δ334 and Δ335 are inactive, mutants Δ336 to Δ345 exhibit significant specific activities and accumulate lactose reasonably well in 60 min (with the exception of mutants Δ336 and Δ345), and mutants Δ346 and Δ347 are essentially inactive. Thus, loop X/XI appears to be about 10 residues in length, extending from Tyr336 to Phe345, and helix X is comprised of 21 residues extending from Val315 to Lys335, both of which are in reasonably good agreement with topology predictions.

Loop XI/XII. Single deletion mutants were constructed from residues Ala369 to Val384 (Figure 1). Mutants Δ369 to Δ373 confer a haloed phenotype on indicator plates, mutants Δ374, Δ375, and Δ376 confer a dark red phenotype, and with the exception of mutant Δ380 which is white, mutants Δ377 to Δ384 exhibit haloed phenotypes. Mutants Δ369 to Δ372 are expressed poorly, mutants Δ373 to Δ379 are expressed to measurable levels, and with the exception of mutant Δ381 which is expressed at about 20% of wild-type, expression of mutants Δ380 to Δ384 is severely compromised (Figure 8). Mutants Δ369 to Δ373 exhibit immeasurably low specific activities. With the exception of mutant Δ377 which displays low activity, mutants Δ374 to Δ381 exhibit high specific activities or accumulate lactose to significant levels in 60 min (note that mutant Δ380 is not expressed) (see *36*). Mutants Δ382 to Δ384 exhibit little or no activity. Finally, although overexpression of the poorly expressed mutants in *E. coli* T184(DE3) leads to a marked increase in the amount of permease in the membrane, activity remains nil (Table 1). The results suggest that loop XI/XII extends from Met372/Tyr374 to Gln379/Ala381, and helix XI is comprised of approximately 27 residues extending from about Ser346 to Met372/Tyr373.

The C Terminus. The C terminus of helix XII is predicted to terminate at Leu400 (Figure 1). Single amino acid deletions were initiated at Ala386 proceeding toward the C terminus to Gly401. Mutants Δ386 to Δ396 grow as haloed colonies, Δ397, Δ399, and Δ401 confer the wild-type red phenotype, and colonies expressing mutant Δ398 are haloed. Consistent with previous observations using engineered truncation mutants at the C terminus of helix XII (*6*−*8*), expression of mutants Δ398 to Δ386 is severely compromised, and Δ400 is not detectable (*37*), while single deletion mutants Δ398, Δ399, and Δ401 (i.e., residues thought to comprise the final turn of helix XII) are expressed at measurable levels (Figure 9). Mutants Δ386 to Δ394 have insignificant activity, and mutants Δ396, Δ397, and Δ398 accumulate lactose to significant levels in 60 min, but specific activities are negligible. Mutants Δ399 and Δ401 accumulate lactose with high specific activities, and by 60 min, levels of accumulation approximate the wild-type. In addition, mutants Δ394, Δ392, Δ390, Δ388, and Δ386 were overexpressed in *E. coli* T184(DE3), and although expression increases markedly, the mutants still exhibit low activity (Table 1). Based primarily on expression levels and the specific activity profiles of the mutants, the C terminus of helix XII is located at Thr399/Leu400, as indicated previously (*1, 6*−*8*). From this analysis, helix XII consists of

approximately 19−22 residues from Gln379/Ala381 to Thr399/Leu400.

DISCUSSION

The use of single deletion analysis to approximate loop−helix boundaries is derived from observations showing that insertion or deletion of residues in putative transmembrane α-helical domains disrupts activity, but is relatively innocuous in extramembanous regions (*29*, *30*, *32*−*34*). By using the approach systematically (*27*), it was shown that deletion of single residues in several periplasmic or cytoplasmic loops has relatively little effect on permease activity. On the other hand, deletion of amino acid residues over a narrow range of positions at or near predicted loop−helix boundaries leads to complete loss of activity. While findings generally consistent with hydropathy analysis were obtained in loops VI/VII, VIII/IX, and IX/X and the flanking helices, deletion analysis of loops III/IV, IV/V, and V/VI and the flanking helices indicates that Glu126 and Arg144 are located within helices IV and V, respectively, rather than at the membrane−water interface at the cytoplasmic face of the membrane (*1*), and a modified secondary structure for the permease was proposed. In this paper, single deletion analysis is applied to the N terminus, the remaining loops, and the C terminus of lac permease.

The findings indicate that the N terminus of helix I approximates Met11/Phe12, which is in reasonable agreement with topology predictions. However, Trp10 is in a hydrophobic environment (*38*) and presumably lies external to the transmembrane helix (Figure 1). Site-directed polyclonal antibodies raised against a peptide corresponding to the N terminus of the permease do not bind to the intact molecule (*39*). Furthermore, when the biotin acceptor domain from a *Klebsiella pneumoniae* oxalacetate decarboxylase is inserted between Thr7 and Asn8, the domain is not biotinylated in vivo (*40*). Thus, the N terminus may be sequestered, and the environment surrounding Trp10 may not specifically reflect location within the membrane. In any event, it is apparent that Trp10 and Trp33 are located at or near the ends of helix I, a finding consistent with the location of these aromatic side chains in many known transmembrane α-helical proteins (*41*).

Truncation of the first 10 amino acids of lac permease results in the loss of expression when the permease is expressed at relatively low levels (*42*). A similar loss is not observed with single deletion mutants. Interestingly, when the permease is overexpressed from a T7 promoter, the first 22 residues can be deleted without abolishing transport activity, indicating that this region of the permease is not required for active transport (*42*). In contrast, important contacts at the periplasmic end of helix I have been demonstrated by mutational analysis and *N*-ethylmaleimide inhibition studies (*43*). Furthermore, specific Cys residues in helix I cross-link with Cys residues in helices VII, XI, and XII (*44*−*47*). Taken together, the loss of activity associated with individual deletion of Phe12 or Gly13 suggests that by changing the pitch of helix I, deletions within the helix may disrupt important distal interactions (*34*).

Loop II/III, containing the conserved Major Facilitor Superfamily motif GXXX(D/E)(R/K)XG(R/K)(R/K) (*48*), is predicted by deletion analysis to contain as few as three to four residues and proposes the placement of ionizable residues within or at the interfaces of transmembrane domains in a fashion similar to that previously shown for loop IV/V by deletion studies (*27*). Loops containing from two to four residues have been described within known membrane protein structures (*49*) and proposed based upon statistical analysis of genomic sequences encoding putative polytopic membrane proteins (*2*). The placement of the ionizable residues within the cytoplasmic regions of helices II, III, IV, and V is consistent with the lack of reactivity of these residues with hydrophilic amino acid-specific reagents (*50*) and with the insensitivity of this region to protease digestion with clostripain in particular (*51*).

The periplasmic end of helix III is predicted to start with Leu99; however, deletion analysis suggests that the N-terminal residue in this helix is Phe91. None of the residues in this transmembrane domain are essential for active transport, and only mutant G96C is significantly inhibited by NEM (*52*), suggesting that this region may make few tertiary contacts. Loss of expression and transport activity of single Ala insertions between residues 89/90, 90/91, and 93/94 does little to elucidate the periplasmic end of helix III (*34*). Accordingly, further work is required to resolve this question.

The most striking observation from this and the preceding work (*27*) is that transmembrane domain VI behaves radically different with respect to deletion analysis from the remainder of the permease. Thus, with the exception of three deletion mutants, Δ172, Δ176, and Δ177, located presumably in the middle of this transmembrane domain which are completely inactive, each of the other deletion mutants in this general region exhibits transport activity, albeit low in some cases. Despite the lack of a consistent pattern with respect to expression or active transport, mutants Δ170 to Δ187 exhibit haloed phenotypes on indicator plates relative to mutants bordering this sequence, suggesting decreased downhill transport activity. Thus, the periplasmic end of this transmembrane domain may differ by four residues from that predicted (Figure 1). The presence of both the N and C termini of lac permease on the cytoplasmic face of the membrane (*4*), the phenotype of phoA−lacY fusions in this region (*3*), and the loss of activity associated with amino acid insertions between residues 177 and 178 (*32*) strongly suggest that putative helix VI spans the membrane. This domain which is proposed to be at the periphery of the 12-helix bundle (*53*) may make few functionally important contacts, thereby accounting for the observations. Regardless, the findings for this region cannot be interpreted in a straightforward manner, and further study by nitroxide-scanning electron paramagnetic resonance, for example, is required before definitive conclusions can be drawn.

Deletion analysis indicates that the C terminus of helix XII approximates Thr399/Leu400, which is in reasonable agreement with topology predictions. Site-directed spin labeling of single Cys mutants from residues 387−402 in helix XII shows a clear pattern of mobility and accessibility to relaxing agent consistent with this region being in a helical conformation (*9*). In addition, replacement of residues 397−400 with four Leu residues yields a stable and functional molecule whereas a construct with Gly-Pro-Gly-Pro at these positions is unstable (*7*). Recent findings indicate that a chymotrypsin-like activity cleaves the C terminus at Phe398/

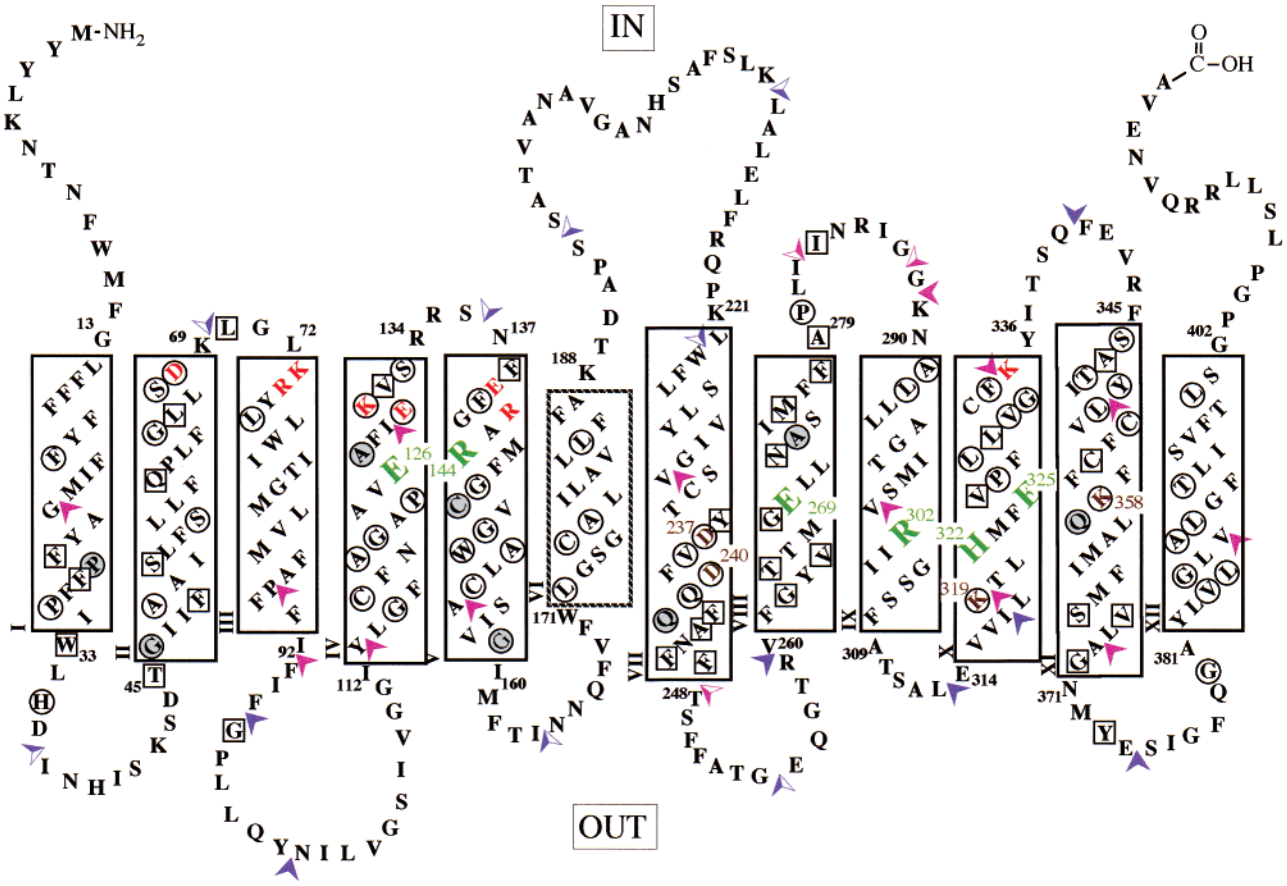

FIGURE 10: Functional secondary structure model of lac permease derived from single deletion analysis. The single-letter amino acid code is used, residues critical for active transport are highlighted in large green type, and the charge pairs Asp237/Lys358 and Asp240/Lys319 are shown in small brown type. Solid rectangles represent helical regions defined by deletion analysis. The dashed helix VI represents the region defined by a decrease in downhill transport assessed by phenotype on indicator media. Orange letters represent ionizable residues predicted within the cytoplasmic ends of transmembrane helices II, III, IV, and V by deletion analysis. Squared residues represent positions where the transport activity of single Cys replacement mutants is inhibited by NEM treatment (*58*). Circled residues represent positions where missense mutations have been shown to inhibit lactose accumulation (*29*, *58*, *59*). Residues in gray circles represent positions where both results have been observed. Two-tone arrowheads indicate locations where discontinuities in the primary sequence have been introduced (*20*, *25*, *57*), and solid arrowheads indicate regions where amino acids have been inserted into the permease (*30*, *32*−*34*). Purple arrowheads indicate good transport activity, and red arrowheads indicate little or no transport activity.

Thr399 (M. Sahin-Tóth and H. R. Kaback, unpublished results), which is also consistent with the results of deletion analysis.

Taken together with the previous findings (*27*), single deletion analysis has been utilized to functionally define both the N and C termini of 11 of the 12 transmembrane regions of lac permease ranging from approximately 18 to 27 residues per helix with an average length of 21 residues (Figure 10), consistent with statistical analysis of predicted transmembrane helices from genomic data (*54*) and analysis of known membrane protein structures (*55*, *56*). A total of 19 of the 22 loop−helix boundaries estimated by deletion analysis are within 3 residues of known or predicted interfaces, suggesting a strong correlation exists between structure and loss of activity as determined by deletion analysis. The proposed model is consistent with findings from insertional mutagenesis (*30*, *32*−*34*), as well as studies on split permease constructs (*20*, *25*, *57*). In addition, deletion of a few residues within loop regions results in the loss of transport activity. Consistent with this finding, over 90% of missense mutations (*29*, *58*, *59*) and alkylation-sensitive Cys replacement mutants (*58*) are localized within helices or at helical interfaces as judged by deletion analysis.

ACKNOWLEDGMENT

We thank Kerstin Stempel for synthesis of oligonucleotides and help in the preparation of figures and Joseph Runner for technical assistance in the construction of the N-terminal deletion mutants.

REFERENCES

1. Foster, D. L., Boublik, M., and Kaback, H. R. (1983) *J. Biol. Chem. 258*, 31−34.
2. Tusnády, G. E., and Simon, I. (1998) *J. Mol. Biol. 283*, 489−506.
3. Calamia, J., and Manoil, C. (1990) *Proc. Natl. Acad. Sci. U.S.A. 87*, 4937−4941.
4. Kaback, H. R. (1996) in *Handbook of Biological Physics: Transport Processes in Eukaryotic and Prokaryotic Organisms* (Konings, W. N., Kaback, H. R., and Lolkema, J. S., Eds.) pp 203−227, Elsevier, Amsterdam.
5. Kwaw, I., Sun, J., and Kaback, H. R. (2000) *Biochemistry 39*, 3134−3140.
6. McKenna, E., Hardy, D., Pastore, J. C., and Kaback, H. R. (1991) *Proc. Natl. Acad. Sci. U.S.A. 88*, 2969−2973.
7. McKenna, E., Hardy, D., and Kaback, H. R. (1992) *J. Biol. Chem. 267*, 6471−6474.
8. Roepe, P. D., Zbar, R. I., Sarkar, H. K., and Kaback, H. R. (1989) *Proc. Natl. Acad. Sci. U.S.A. 86*, 3992−3996.

9. Voss, J., He, M., Hubbell, W., and Kaback, H. R. (1996) *Biochemistry 35*, 12915−12918.
10. Sun, J., Wu, J., Carrasco, N., and Kaback, H. R. (1996) *Biochemistry 35*, 990−998.
11. Sun, J., Frillingos, S., and Kaback, H. R. (1997) *Protein Sci. 6*, 1503−1510.
12. Voss, J., Hubbell, W. L., Hernandez, J., and Kaback, H. R. (1997) *Biochemistry 36*, 15055−15061.
13. King, S. C., Hansen, C. L., and Wilson, T. H. (1991) *Biochim. Biophys. Acta 1062*, 177−186.
14. Sahin-Tóth, M., Dunten, R. L., Gonzalez, A., and Kaback, H. R. (1992) *Proc. Natl. Acad. Sci. U.S.A. 89*, 10547−10551.
15. Lee, J. L., Hwang, P. P., Hansen, C., and Wilson, T. H. (1992) *J. Biol. Chem. 267*, 20758−20764.
16. Dunten, R. L., Sahin-Tóth, M., and Kaback, H. R. (1993) *Biochemistry 32*, 3139−3145.
17. Sahin-Tóth, M., and Kaback, H. R. (1993) *Biochemistry 32*, 10027−10035.
18. Frillingos, S., and Kaback, H. R. (1996) *Biochemistry 35*, 13363−13367.
19. Voss, J., Sun, J., and Kaback, H. R. (1998) *Biochemistry 37*, 8191−8196.
20. Zen, K. H., McKenna, E., Bibi, E., Hardy, D., and Kaback, H. R. (1994) *Biochemistry 33*, 8198−8206.
21. Ujwal, M. L., Jung, H., Bibi, E., Manoil, C., Altenbach, C., Hubbell, W. L., and Kaback, H. R. (1995) *Biochemistry 34*, 14909−14917.
22. Frillingos, S., Gonzalez, A., and Kaback, H. R. (1997) *Biochemistry 36*, 14284−14290.
23. Sahin-Tóth, M., le Coutre, J., Kharabi, D., le Maire, G., Lee, J. C., and Kaback, H. R. (1999) *Biochemistry 38*, 813−819.
24. Venkatesan, P., and Kaback, H. R. (1998) *Proc. Natl. Acad. Sci. U.S.A. 95*, 9802−9807.
25. Wolin, C. D., and Kaback, H. R. (2000) *Biochemistry 39*, 6130−6135.
26. Zhao, M., Zen, K.-C., Hubbell, W., and Kaback, H. R. (1999) *Biochemistry 38*, 7407−7412.
27. Wolin, C., and Kaback, H. R. (1999) *Biochemistry 38*, 8590−8597.
28. Zhao, M., Zen, K.-C., Hernandez-Borrell, J., Altenbach, C., Hubbell, W. L., and Kaback, H. R. (1999) *Biochemistry 38*, 15970−15977.
29. Bailey, J., and Manoil, C. (1998) *J. Mol. Biol. 277*, 199−213.
30. Goswitz, V. C., Matzke, E. A., Taylor, M. R., Jessen-Marshall, A. E., and Brooker, R. J. (1996) *J. Biol. Chem. 271*, 21927−21932.
31. Hong, K. H., and Miller, C. (2000) *J. Gen. Physiol. 115*, 51−58.
32. Manoil, C., and Bailey, J. (1997) *J. Mol. Biol. 267*, 250−263.
33. McKenna, E., Hardy, D., and Kaback, H. R. (1992) *Proc. Natl. Acad. Sci. U.S.A. 89*, 11954−11958.
34. Braun, P., Persson, B., Kaback, H. R., and von Heijne, G. (1997) *J. Biol. Chem. 272*, 29566−29571.
35. Carrasco, N., Herzlinger, D., Mitchell, R., DeChiara, S., Danho, W., Gabriel, T. F., and Kaback, H. R. (1984) *Proc. Natl. Acad. Sci. U.S.A. 81*, 4672−4676.
36. Jung, K., Jung, H., Colacurcio, P., and Kaback, H. R. (1995) *Biochemistry 34*, 1030−1039.
37. He, M. M., Sun, J., and Kaback, H. R. (1996) *Biochemistry 35*, 12909−12914.
38. Weitzman, C., Consler, T. G., and Kaback, H. R. (1995) *Protein Sci. 4*, 2310−2318.
39. Carrasco, N., Herzlinger, D., Dechiara, S., Danho, W., and Kaback, H. R. (1985) *Ann. N.Y. Acad. Sci. 456*, 305−306.
40. Zen, K., Consler, T. G., and Kaback, H. R. (1995) *Biochemistry 34*, 3430−3437.
41. Yau, W. M., Wimley, W. C., Gawrisch, K., and White, S. H. (1998) *Biochemistry 37*, 14713−14718.
42. Bibi, E., Stearns, S. M., and Kaback, H. R. (1992) *Proc. Natl. Acad. Sci. U.S.A. 89*, 3180−3184.
43. Sahin-Tóth, M., Persson, B., Schwieger, J., Cohan, M., and Kaback, H. R. (1994) *Protein Sci. 3*, 240−247.
44. Wu, J., and Kaback, H. R. (1996) *Proc. Natl. Acad. Sci. U.S.A. 93*, 14498−14502.
45. Wu, J., and Kaback, H. R. (1997) *J. Mol. Biol. 270*, 285−293.
46. Wu, J., Hardy, D., and Kaback, H. R. (1998) *Biochemistry 37*, 15785−15790.
47. Wang, Q., and Kaback, H. R. (1999) *J. Mol. Biol. 291*, 683−692.
48. Henderson, P. J. (1990) *J. Bioenerg. Biomembr. 22*, 525−569.
49. Monné, M., Nilsson, I., Elofsson, A., and von Heijne, G. (1999) *J. Mol. Biol. 293*, 807−814.
50. Page, M. G., and Rosenbusch, J. P. (1988) *J. Biol. Chem. 263*, 15906−15914.
51. Stochaj, U., Bieseler, B., and Ehring, R. (1986) *Eur. J. Biochem. 158*, 423−428.
52. Sahin-Tóth, M., Frillingos, S., Bibi, E., Gonzalez, A., and Kaback, H. R. (1994) *Protein Sci. 3*, 2302−2310.
53. Sun, J., and Kaback, H. R. (1997) *Biochemistry 36*, 11959−11965.
54. Arkin, I. T., and Brunger, A. T. (1998) *Biochim. Biophys. Acta 1429*, 113−128.
55. Bowie, J. U. (1997) *J. Mol. Biol. 272*, 780−789.
56. Wallin, E., Tsukihara, T., Yoshikawa, S., von Heijne, G., and Elofsson, A. (1997) *Protein Sci. 6*, 808−815.
57. Bibi, E., and Kaback, H. R. (1990) *Proc. Natl. Acad. Sci. U.S.A. 87*, 4325−4329.
58. Frillingos, S., Sahin-Tóth, M., Wu, J., and Kaback, H. R. (1998) *FASEB J. 12*, 1281−1299.
59. Stewart, C., Bailey, J., and Manoil, C. (1998) *J. Biol. Chem. 273*, 28078−28084.

BI0025767